Research Article | Vol. 26, No. 13 | 25 Jun 2018 | OPTICS EXPRESS 17563
Optics EXPRESS

Control the orbital angular momentum in third-harmonic generation using quasi-phase-matching

ZHOU XU,[1] ZHONGYU LIN,[1] ZHILIN YE,[1] YAN CHEN,[1] XIAOPENG HU,[1,*] YAODONG WU,[1] YONG ZHANG,[2,4] PENG CHEN,[2] WEI HU,[2] YANQING LU,[2] MIN XIAO,[1,2,3] AND SHINING ZHU[1]

[1]*National Laboratory of Solid State Microstructures and School of Physics, Nanjing University, Nanjing 210093, China*
[2]*College of Engineering and Applied Sciences, Nanjing University, Nanjing 210093, China*
[3]*Department of Physics, University of Arkansas, Fayetteville, Arkansas 72701, USA*
[4]*zhangyong@nju.edu.cn*
[*]*xphu@nju.edu.cn*

Abstract: Manipulating photon's orbital angular momentum (OAM) through nonlinear interactions has drawn increasing research interests in recent years. In this work, we propose a scheme to control the OAM of the third harmonic wave through two cascaded second-order nonlinear processes. A Gaussian beam was frequency doubled at the first stage. Subsequent sum frequency mixing of the Gaussian second harmonic wave and an orthogonal-polarized Laguerre-Gaussian-like fundamental wave generate the third harmonic wave, which carries the same OAM as that of the Laguerre-Gaussian-like fundamental wave. In this experiment, we demonstrated controlling the OAM of the third harmonic wave in a tandem periodically-poled $LiTaO_3$ optical superlattice, and the results are in accordance with theoretical predictions.

OCIS codes: (080.4865) Optical vortices; (190.2620) Harmonic generation and mixing; (160.4330) Nonlinear optical materials.

References and links

1. L. Allen, M. W. Beijersbergen, R. J. C. Spreeuw, and J. P. Woerdman, "Orbital angular momentum of light and the transformation of Laguerre-Gaussian laser modes," Phys. Rev. A **45**(11), 8185–8189 (1992).
2. M. J. Padgett, "Orbital angular momentum 25 years on [Invited]," Opt. Express **25**(10), 11265–11274 (2017).
3. B. Thidé, H. Then, J. Sjöholm, K. Palmer, J. Bergman, T. D. Carozzi, Y. N. Istomin, N. H. Ibragimov, and R. Khamitova, "Utilization of photon orbital angular momentum in the low-frequency radio domain," Phys. Rev. Lett. **99**(8), 087701 (2007).
4. Z. Y. Zhou, S. L. Liu, Y. Li, D. S. Ding, W. Zhang, S. Shi, M. X. Dong, B. S. Shi, and G. C. Guo, "Orbital angular momentum-entanglement frequency transducer," Phys. Rev. Lett. **117**(10), 103601 (2016).
5. D. G. Grier, "A revolution in optical manipulation," Nature **424**(6950), 810–816 (2003).
6. S. W. Hell and J. Wichmann, "Breaking the diffraction resolution limit by stimulated emission: stimulated-emission-depletion fluorescence microscopy," Opt. Lett. **19**(11), 780–782 (1994).
7. A. Mair, A. Vaziri, G. Weihs, and A. Zeilinger, "Entanglement of the orbital angular momentum states of photons," Nature **412**(6844), 313–316 (2001).
8. J. Wang, J. Y. Yang, I. M. Fazal, N. Ahmed, Y. Yan, H. Huang, Y. Ren, Y. Yue, S. Dolinar, M. Tur, and A. E. Willner, "Terabit free-space data transmission employing orbital angular momentum multiplexing," Nat. Photonics **6**(7), 488–496 (2012).
9. M. P. J. Lavery, C. Peuntinger, K. Günthner, P. Banzer, D. Elser, R. W. Boyd, M. J. Padgett, C. Marquardt, and G. Leuchs, "Free-space propagation of high-dimensional structured optical fields in an urban environment," Sci. Adv. **3**(10), e1700552 (2017).
10. F. Steinlechner, N. Hermosa, V. Pruneri, and J. P. Torres, "Frequency conversion of structured light," Sci. Rep. **6**(1), 21390 (2016).
11. R. Ni, Y. F. Niu, L. Du, X. P. Hu, Y. Zhang, and S. N. Zhu, "Topological charge transfer in frequency doubling of fractional orbital angular momentum state," Appl. Phys. Lett. **109**(15), 151103 (2016).
12. H. Li, H. G. Liu, and X. F. Chen, "Nonlinear vortex beam array generation by spatially modulated fundamental wave," Opt. Express **25**(23), 28668–28673 (2017).

#330166 https://doi.org/10.1364/OE.26.017563
Journal © 2018 Received 24 Apr 2018; revised 5 Jun 2018; accepted 18 Jun 2018; published 21 Jun 2018

Optics EXPRESS

13. Z. Y. Zhou, D. S. Ding, Y. K. Jiang, Y. Li, S. Shi, X. S. Wang, and B. S. Shi, "Orbital angular momentum light frequency conversion and interference with quasi-phase matching crystals," Opt. Express **22**(17), 20298–20310 (2014).
14. K. Miyamoto, S. Miyagi, M. Yamada, K. Furuki, N. Aoki, M. Okida, and T. Omatsu, "Optical vortex pumped mid-infrared optical parametric oscillator," Opt. Express **19**(13), 12220–12226 (2011).
15. A. Aadhi, G. K. Samanta, S. Chaitanya Kumar, and M. Ebrahim-Zadeh, "Controlled switching of orbital angular momentum in an optical parametric oscillator," Optica **4**(3), 349–355 (2017).
16. D. S. Ding, Z. Y. Zhou, B. S. Shi, X. B. Zou, and G. C. Guo, "Linear up-conversion of orbital angular momentum," Opt. Lett. **37**(15), 3270–3272 (2012).
17. G. Walker, A. S. Arnold, and S. Franke-Arnold, "Trans-spectral orbital angular momentum transfer via four-wave mixing in Rb vapor," Phys. Rev. Lett. **108**(24), 243601 (2012).
18. M. Zurch, C. Kern, P. Hansinger, A. Dreischuh, and Ch. Spielmann, "Strong-field physics with singular light beams," Nat. Phys. **8**(10), 743–746 (2012).
19. N. V. Bloch, K. Shemer, A. Shapira, R. Shiloh, I. Juwiler, and A. Arie, "Twisting light by nonlinear photonic crystals," Phys. Rev. Lett. **108**(23), 233902 (2012).
20. N. Apurv Chaitanya, S. Chaitanya Kumar, K. Devi, G. K. Samanta, and M. Ebrahim-Zadeh, "Ultrafast optical vortex beam generation in the ultraviolet," Opt. Lett. **41**(12), 2715–2718 (2016).
21. X. Fang, G. Yang, D. Wei, D. Wei, R. Ni, W. Ji, Y. Zhang, X. Hu, W. Hu, Y. Q. Lu, S. N. Zhu, and M. Xiao, "Coupled orbital angular momentum conversions in a quasi-periodically poled $LiTaO_3$ crystal," Opt. Lett. **41**(6), 1169–1172 (2016).
22. Y. Wu, R. Ni, Z. Xu, Y. Wu, X. Fang, D. Wei, X. Hu, Y. Zhang, M. Xiao, and S. Zhu, "Tunable third harmonic generation of vortex beams in an optical superlattice," Opt. Express **25**(25), 30820–30826 (2017).
23. X. P. Hu, P. Xu, and S. N. Zhu, "Engineered quasi-phase-matching for laser techniques [Invited]," Photon. Res. **1**(4), 171–185 (2013).
24. A. Arie and N. Voloch, "Periodic, quasi-periodic, and random quadratic nonlinear photonic crystals," Laser Photonics Rev. **4**(3), 355–373 (2010).
25. K. S. Abedin and H. Ito, "Temperature-dependent dispersion relation of ferroelectric lithium tantalite," J. Appl. Phys. **80**(11), 6561–6563 (1996).
26. S. N. Zhu, Y. Y. Zhu, Z. Y. Zhang, H. Shu, H. F. Wang, J. F. Hong, C. Z. Ge, and N. B. Ming, "$LiTaO_3$ crystal periodically poled by applying an external pulsed field," J. Appl. Phys. **77**(10), 5481–5483 (1995).
27. P. Vaity, J. Banerji, and R. P. Singh, "Measuring the topological charge of an optical vortex by using a tilted convex lens," Phys. Lett. A **377**(15), 1154–1156 (2013).
28. G. D. Xu, T. W. Ren, Y. H. Wang, Y. Y. Zhu, S. N. Zhu, and N. B. Ming, "Third-harmonic generation by use of focused Gaussian beams in an optical superlattice," J. Opt. Soc. Am. B **20**(2), 360–365 (2003).
29. I. Shoji, T. Kondo, A. Kitamoto, M. Shirane, and R. Ito, "Absolute scale of second-order nonlinear-optical coefficients," J. Opt. Soc. Am. B **14**(9), 2268–2294 (1997).
30. Z. Y. Zhou, Y. Li, D. S. Ding, W. Zhang, S. Shi, B. S. Shi, and G. C. Guo, "Orbital angular momentum photonic quantum interface," Light Sci. Appl. **5**(1), e16019 (2016).
31. P. Chen, L. L. Ma, W. Duan, J. Chen, S. J. Ge, Z. H. Zhu, M. J. Tang, R. Xu, W. Gao, T. Li, W. Hu, and Y. Q. Lu, "Digitalizing Self-Assembled Chiral Superstructures for Optical Vortex Processing," Adv. Mater. **30**(10), 1705865 (2018).
32. W. Ji, C. H. Lee, P. Chen, W. Hu, Y. Ming, L. Zhang, T. H. Lin, V. Chigrinov, and Y. Q. Lu, "Meta-q-plate for complex beam shaping," Sci. Rep. **6**(1), 25528 (2016).

1. Introduction

Light beams whose spatial waveform feature an azimuthal phase dependence of the form $\exp(-il\theta)$, carry an OAM of $l\hbar$ per photon [1], where θ is the azimuthal coordinate in the transverse plane and the integer l is the topological charge (TC). The unique properties related to the OAM make such beams an intensively studied topic with diverse applications in micromanipulation, super-resolution imaging, classical and quantum communications [2–9]. Among these studies, the OAM exchange in nonlinear interactions is of particular interest. Through frequency conversion, such as the frequency up [10–13] and down conversions [14,15] in nonlinear optical crystals, four wave mixing in atomic vapor [16,17], and high harmonic generation (HHG) in a gas medium [18], light beams carrying OAM could be generated at new wavelengths. During frequency conversions of OAM-carrying beams, arithmetic relations among the TC of the interacting modes are generally satisfied, i.e., the TC of the harmonic wave is equal to that of the fundamental wave (FW) multiplied by the harmonic order. However, in practical applications, such as stimulated emission depletion microscopy, light beams carrying certain OAM at the target wavelength are preferred. In an optical parametric oscillation, the OAM of the pump can be selectively transferred to the

Optics EXPRESS

generated beams by controlling the relative losses of the resonant beams [15]. Second harmonic (SH) waves with arbitrary OAMs were obtained at different diffraction orders from twisted quadratic nonlinear crystals [19]. Third harmonic generation (THG) and fourth harmonic generation can transfer OAM from the commercially available near-infrared laser to short wavelength (down to the ultraviolet) through cascaded processes in second-order nonlinear crystals [20–22]. For example, in our previous work [21], near-infrared light carrying OAM was converted to the visible through THG in a quasi-periodical optical superlattice and the OAM of the third harmonic (TH) wave was three times that of the FW. In such high-harmonic generations which based on cascaded second-order nonlinearity, methods to control the OAM of the generated harmonic waves regardless of the harmonic order remains an interesting topic.

In this paper, we propose a scheme to control the OAM in THG using quasi-phase-matching (QPM). The FWs consist of Gaussian and Laguerre-Gaussian-like (LG-like) beams with the same frequency. Firstly, the Gaussian beam is converted into SH wave with a Gaussian profile. Subsequently, sum frequency mixing of the Gaussian-shaped SH wave and the LG-like FW generates the TH wave carrying the same OAM as that of the LG-like FW. Currently, it is still a challenge to separate beams carrying different OAMs with the same frequency and same polarization. In the proposed scheme, we utilized the polarization degree of freedom, and set the two FWs at different polarizations. By choosing suitable nonlinear frequency converters, in which the individual THG of the input FWs should not occur, a pure output of the OAM-controlled TH wave may be obtained. The cascaded processes can be realized using two birefringent crystals based on birefringence phase matching. In contrast, an optical superlattice based on QPM can provide access to the largest nonlinear coefficient of the material and avoid spatial walk-off. Most importantly, it is feasible to arrange for multiple parametric interactions in a single crystal by domain engineering [23, 24]. The nonlinear optical material used in our experiment is a tandem periodically poled $LiTaO_3$ crystal with two cascaded domain sections. The first section of the superlattice was used for frequency doubling of the extraordinary Gaussian beam. The second part was used for sum frequency mixing of the extraordinary SH wave and ordinary LG-like beam at the fundamental frequency, generating the ordinary TH wave carrying the same OAM as that of the input LG-like FW, as indicated in Fig. 1.

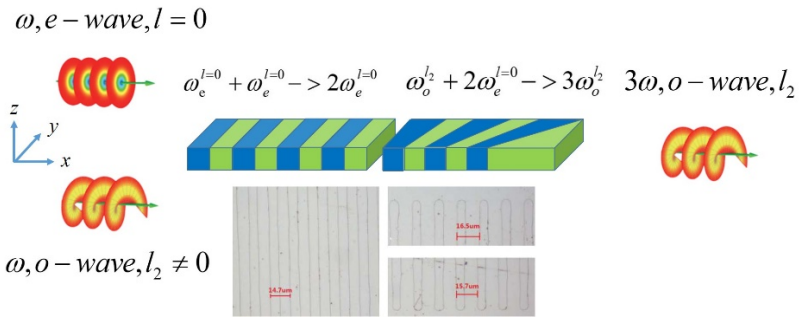

Fig. 1. Illustration of the scheme for controlling the OAM of the TH wave in an optical superlattice. The inset is the microphotograph of the domain structures revealed by etching. The left part of the inset corresponds to the first periodic structure of the superlattice. The upper-right and lower-right parts of the inset are the corresponding parts of the fan-out domain structure in the second section.

In this work, we chose congruent $LiTaO_3$ (CLT) as the host material. In comparison with other materials, such as congruent $LiNbO_3$ and KTP, CLT has a high damage threshold and a relative simple poling technique. The poling period of the first part was 14.7 um, which was used for first order SHG of 1342 nm via a type-0 (eee) phase-matching process at 100 °C. In order to compensate for the inaccuracy of the Sellmeier Equation of CLT crystals [25], the

Optics EXPRESS

second part had a fan-out structure in which the poling periods varied from 15.7 to 16.5 μm, which was used for the third-order sum frequency mixing of the 671 nm extraordinary wave and 1342 nm ordinary wave through a type-II (eoo) process. The optical superlattice was fabricated using the conventional electrical-field poling technique [26] and the lengths of the two sections were 10 and 8 mm. The microphotographs of the domain structures revealed by etching are as shown in Fig. 1; the inverted domain distributions were uniform in both sections and the duty cycles of the two sections were 50% and 40% respectively.

2. Experimental setup

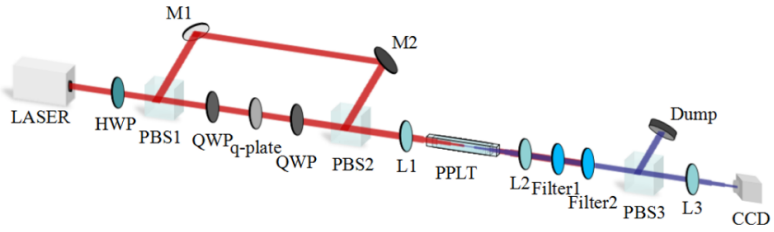

Fig. 2. Schematic of the experimental setup.

The schematic of the experimental setup is shown in Fig. 2. The fundamental light source was a watt-level diode-pumped Nd:YVO_4 laser working at 1342 nm with a 10 kHz repetition rate and a 50 ns pulse duration. The polarization of the z-polarized FW from the laser was rotated by 40° using a half-wave plate. Then the FW was split into two branches with a polarizing beam splitter (PBS). The z-polarized FW in the upper branch had a Gaussian-shaped intensity profile. The OAM was imprinted onto the y-polarized FW in the lower branch through spin-to-orbital conversion using a quarter wave-plate (QWP) together with a q-plate. The circularly polarized OAM-carrying FW was then transformed to linear y-polarization using a second QWP. The two beams were then recombined and focused into the optical superlattice using a lens with the focusing length of 50 mm. The optical path difference of the un-balanced Mach-Zehnder interferometer was 15 cm, and the time delay between the pulses from the two arms was calculated to be 0.5 ns, which is negligible in comparison with the pulse duration of 50 ns. The optical superlattice was placed in an oven for temperature control. After filtering the residual FWs and generated red light with two filters, the profile of the generated TH wave at 447 nm was detected with a CCD. To reveal the TC of the beams, a titled convex lens was used to convert the LG modes to Hermite-Gaussian modes. By counting the dark strips in the converted pattern, we obtained the TC of the OAM state [27].

3. Results and discussions

To characterize the SHG part of the nonlinear crystal, only a z-polarized Gaussian beam at 1342 nm was incident onto the nonlinear crystal. The measured optimal phase-matching temperature of the SHG in the first section was 105.5 °C, and the deviation from the designed value of 100 °C was attributed to the inaccuracy of the Sellmeier Equation of CLT as well as small fabrication errors during sample fabrication. A maximum output power of 550 mW was obtained with a 1.1-W input. Taking into account the Fresnel reflection loss which is about 13% at the facet of the optical superlattice, the SHG efficiency was about 66%. High efficiency SHG can be described using the coupled-wave equations for focused Gaussian beams in [28]:

$$\begin{aligned}\frac{dA_1(x)}{dx} &= -\frac{i}{\sqrt{b}(1+i\xi)}[aA_2A_1^*\exp(-i\Delta kx)]\\ \frac{dA_2(x)}{dx} &= -\frac{i}{2\sqrt{b}(1-i\xi)}[aA_1^2\exp(i\Delta kx)],\end{aligned} \tag{1}$$

Optics EXPRESS

with

$$\xi = \frac{2x}{b}, \tag{2}$$

$$a = d_{33} f_m [\frac{\omega_1^3 \omega_2}{(\pi c)^3 n_1 n_2}]^{1/2}, \tag{3}$$

where A_j, ω_j, n_j are the field amplitudes, angular frequencies, and refractive indices of the FW and SH wave respectively. $\Delta k = k_2 - 2k_1 - G_m$ is the wave-vector mismatch between the FW (k_1) and the SH wave (k_2), and this wave-vector mismatch can be compensated by the mth-order reciprocal vector $G_m = 2m\pi / \Lambda$ provided by the optical superlattice with a poling period of Λ. $b = k_j W_{0j}^2, j = 1,2$ is the confocal parameter where W_{0j} are the waist radii of Gaussian beams. $f_m = 2\sin(m\pi D)/(m\pi)$ is the Fourier coefficient of the optical superlattice with D being the duty cycle. c is the speed of light in vacuum. Substituting $W_{01} = \sqrt{2} W_{02} = 40\mu m$, $D = 50\%$ and $d_{33} = 10.7 pm/V$ [29] into Eq. (1), the coupled-wave equations can be numerically solved and the results are shown in Fig. 3. The calculated output power of the SH wave at the end facet of the crystal was 670 mW, with a conversion efficiency of ~70%. The measured efficiency is very close to the calculated one which indicates a uniform domain quality in the first section of the optical superlattice.

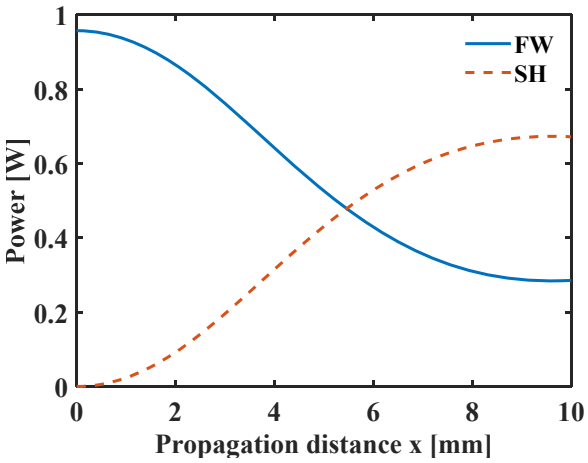

Fig. 3. Dependence of the powers of the FW and SH wave on the propagation distance inside the optical superlattice.

Blue light at 447 nm with z-polarization was observed during the experiment, and the output power was 36 μW. By calculation, we found that the poling period for type-0 sum frequency mixing of 1342-nm near-infrared light and 671-nm red light using the third-order reciprocal vector is 14.682 μm. This poling period is very close to the period (14.7 μm) of the first section, and deviates far from the period (15.7-16.5 μm) of the second part, indicating that z-polarized blue light was not generated from the second part (this was also confirmed by incident the z-polarized FW from the end facet of the second section). In the experiment, the un-wanted z-polarized blue light could be easily separated from the y-polarized blue light using a PBS. To avoid THG of the z-polarized blue light, we can change the phase-matching temperature away from 100°C during the design of the structure of the optical superlattice.

Optics EXPRESS

The SHG of the y-polarized FW was weak in the experiment due to the large wave-vector mismatch, hence THG contained only y-polarized FW was too weak to be observed.

Sum frequency mixing of the z-polarized 671 nm red light (pump) from the first section and the y-polarized 1342 nm near-infrared light (signal) was realized in the second section of the optical superlattice. In the un-depleted pump approximation, the sum frequency generation (SFG) process can be predicted according to [30]:

$$P_{SFG} = \frac{16\pi^2 d_{eff}^2 P_p P_s L^2 l}{\varepsilon_0 c n_S n_{SFG} \lambda_{SFG}^2 \lambda_p} h(l,\xi), \tag{4}$$

with

$$h(l,\xi) = \frac{1}{\xi}\int_{1.25\xi}^{3.25\xi} dx \int_{1.25\xi}^{3.25\xi} dy \frac{(1+ix)^l (1-iy)^l}{\{(1+ix)(1-iy)[2+\frac{i(x-y)}{\beta}] + \alpha(1+\frac{ix}{\beta})(1-\frac{iy}{\beta})[2+i(x-y)]\}^{l+1}}. \tag{5}$$

The upper and lower limits of integration in Eq. (5) are different from which in [30], because the beam waist of the interacting waves were not at the middle of the second section of the optical superlattice. The detailed description of the parameters can be found in the supplementary material of [30].

To characterize the SFG section, firstly, the near-infrared light from the laser passed through a half-wave plate, thus two Gaussian FWs with orthogonal polarization were obtained. The powers of the z-polarized and y-polarized FWs at 1342 nm were 0.68 and 0.48 W respectively, and the power of the SH wave at 671 nm was calculated to be 320 mW according to Eq. (1). Thus some key parameters used in the simulation can be determined and given in the following: $P_p = 735W$ and $P_s = 835W$ (Fresnel loss considered) are the peak powers of the pump and signal waves respectively; $d_{eff} = d_{31} \cdot 2\sin(3\pi D)/(3\pi) = 0.12 pm/V$ is the effective nonlinear coefficient; $\xi = 0.4906$ is the focusing parameter; α=1 / 2 ; β=1.02 . Optimized TH output was obtained by moving the sample along the transverse direction of the fan-out structure. The power of the generated Gaussian TH wave was measured to be 350 μW, which was close to the theoretical value of 400 μW calculated using Eq. (4).

When two FWs with different spatial modes were incident onto the optical superlattice using the un-balanced Mach-Zehnder interferometer, OAM-controlled TH wave could be obtained. We imprinted three different TC numbers, l = 1, 2, and 3, on the y-polarized 1342-nm FW with a liquid crystal q-plate [31, 32]. The intensity profiles and TC numbers of the FW are as shown in Fig. 4(a) and 4(b). Through controlled THG, we can see from Fig. 4(c) that the generated TH waves had doughnut-shaped intensity profiles, and the measured TCs of the TH waves were 1, 2, and 3 using a tilted convex lens, as shown in Fig. 4(d). The results indicate that the OAM of the y-polarized FW wave was transferred to the blue light through THG.

Optics EXPRESS

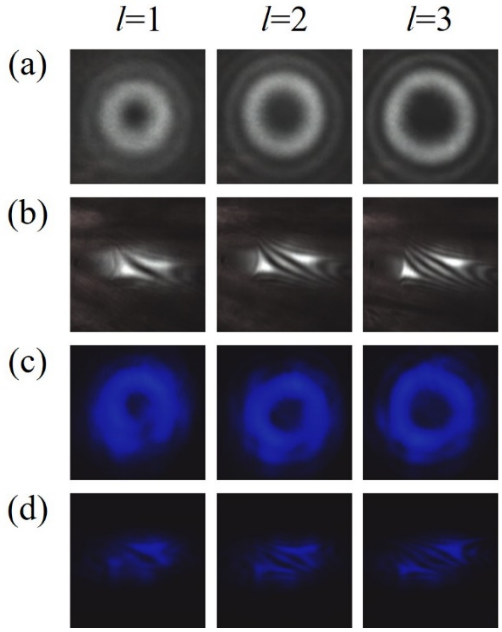

Fig. 4. Intensity profiles of the FW (a) and the generated TH waves (c) recorded by a CCD. By using a titled convex lens, the converted patterns indicate that the TH waves (d) carrying the same OAM as that of the corresponding FWs (b). From left to right, the TC numbers are l = 1, 2 and 3.

Average output powers of 12, 10, and 6 μW at 447 nm were obtained when the TC of the y-polarized FW was 1, 2, and 3 respectively. The conversion efficiency from the total input power to the TH power was of the order 10^{-6}. The measured and theoretical results of the normalized TH power depending on the OAM index of the LG-like FW are shown in Fig. 5. The measured results show a decreasing tendency with increasing OAM index, however, there is a large deviation between experiment and theory for l = 1. This can be explained by the misalignment of the two incident FWs in space when switching to different q-plates, and subsequent a deviation of the nonlinear spatial overlapping integral.

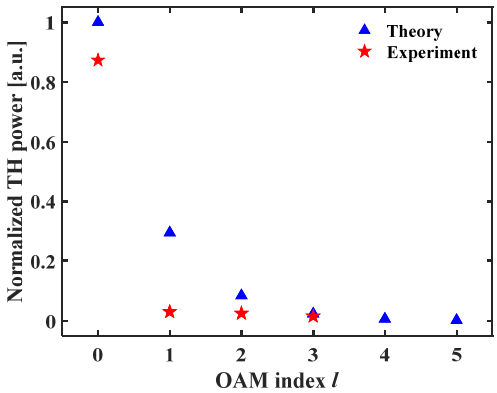

Fig. 5. Measured results and theoretical predictions of the normalized output power of the TH varying with the OAM index of the LG-like fundamental wave.

The temperature tuning waves for the cascaded SHG and SFG processes are shown in Fig. 6; the TC of the y-polarized wave was l = 1. The measured phase-matching temperatures for

Optics EXPRESS

SHG and SFG were both at 105.5 °C, with the full widths at half maximum of 6 and 3.5 °C respectively. Due to the fan-out structure in the second section, the temperature tuning curves of the two processes overlapped well, which is favorable for efficient THG. According to [25], the dispersion of CLT crystal is temperature dependent, so the wave-vector mismatch of the interacting waves in THG will vary with the temperature. Thus the conversion efficiencies of the nonlinear optical processes will change with the temperature of the nonlinear crystal. By numerically solving the coupled-wave equations for THG in [28], the output powers of the SH and TH waves depending on the temperature of the optical superlattice can be fitted, as shown in Fig. 6.

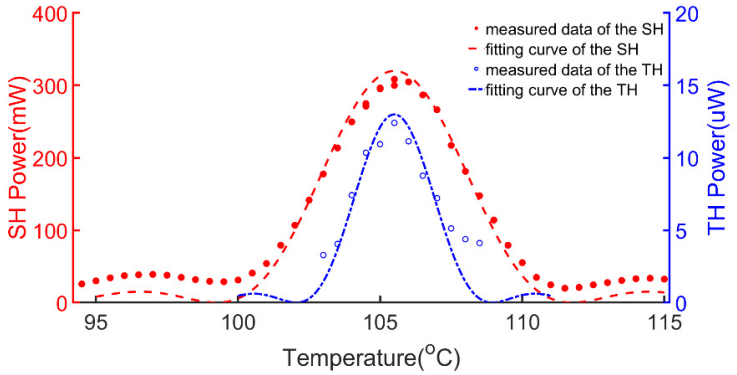

Fig. 6. Measured and fitted temperature tuning curves for the SHG and SFG processes.

4. Conclusions

Two orthogonally polarized waves with the same frequency but different spatial modes were mixed in a tandem periodically-poled $LiTaO_3$ optical superlattice. Through two cascaded nonlinear processes, the TC of the generated TH blue light at 447 nm was equal to that of the input LG-like near-infrared beam at 1342 nm. By carefully designing the domain structure of the optical superlattice, the temperature tuning curves for the cascaded processes overlapped well, and the TH wave with controlled OAM can be separated from those with different spatial modes by polarization filters. The dependence of the output power on the TC of the input wave as well as the conversion efficiency were measured and investigated theoretically. The proposed scheme in this work provides a compact solution for generating light beams carrying desired OAM at short wavelength, and can be further extended to HHG in second-order nonlinear optical materials.

Funding

National Key R&D Program of China (2017YFA0303700); National Natural Science Foundation of China (NSFC) (11674171, 91636106, 11627810, and 11621091); Fundamental Research Funds for the Central Universities (020414380064); Jiangsu Science Foundation (BK20151374); and PAPD of Jiangsu Higher Education Institutions.